

Preparation of Ag/PVP Nanocomposites as a Solid Precursor for Silver Nanocolloids Solution

Hyun-Ki Hong, Chan-Kyo Park,[†] and Myoung-Seon Gong^{*}

Department of Nanobiomedical Science and WCU Research Center of Nanobiomedical Science, Dankook University, Cheonan, Chungnam 330-714, Korea. *E-mail: msgong@dankook.ac.kr

[†]Department of Applied Chemical Engineering, Dankook University, Chungnam 330-714, Korea

Received October 21, 2009, Accepted March 8, 2010

A polyvinylpyrrolidone (PVP)/Ag nanocomposites was prepared by the simultaneous thermal reduction and radical polymerization route. The *in situ* synthesis of the Ag/PVP nanocomposites is based on the finding that the silver *n*-propylcarbamate (Ag-PCB) complex can be directly dissolved in the NVP monomer, and decomposed by only heat treatment in the range of 110 to 130 °C to form silver metal. Silver nanoparticles with a narrow size distribution (5 - 40 nm) were obtained, which were well dispersed in the PVP matrix. A successful synthesis of Ag/PVP nanocomposites then proceeded upon heat treatment as low as 110 °C. Moreover, important advantages of the *in situ* synthesis of Ag/PVP composites include that no additives (e.g. solvent, surface-active agent, or reductant of metallic ions) are used, and that the stable silver nanocolloid solution can be directly prepared in high concentration simply by dissolving the Ag/PVP nanocomposites in water or organic solvent.

Key Words: Silver alkylcarbamate, Silver/PVP, Nanocomposites, Radical polymerization

Introduction

Nanocomposites of metallic and inorganic nanoparticles embedded within a polymer matrix have attracted a great deal of interest for their broad range of potential applications.¹⁻⁴ These materials have bulk properties that are improved over those of the base polymers. The properties of these nanohybrids are dependent on particle size,^{5,6} particle distribution,⁶⁻⁹ and particle density.⁶ Therefore, control of these parameters has been the subject of intensive investigations.

Many synthetic approaches have been applied to the preparation of metal/polymer nanocomposites.¹⁰⁻¹² Conventionally, the polymerization of monomers and formation of metal nanoparticles are performed separately, and then the polymer and nanoparticles are mechanically mixed to form nanocomposites.¹³ However, it is extremely difficult to disperse the nanoparticles homogeneously into the polymer matrix, due to the easy agglomeration of the nanoparticles and the high viscosity of the polymer. In recent years, more attention has been paid to the *in situ* synthesis of metal nanoparticles in polymer matrices. This method is based on the reduction of metal ions that are dispersed in polymer matrices. Many polymer thin films, containing noble metal nanoparticles, have been prepared by reducing polymer metal chelate films such as polyaniline/Au, poly(vinyl alcohol)/Ag, poly(acrylic acid)/Cu.¹⁴⁻¹⁶ The use of silver organic complexes has also been reported as a new method of obtaining silver nanoparticles and conductive silver tracks and coatings, where silver carboxylate¹⁷ and silver alkylcarbamate complexes^{18,19} are reduced to silver metal simply by heating.²⁰⁻²⁶

The most consistently-used material for the stabilization of silver nanoparticles is a polymer, such as PVP, with metal nanoparticles. PVP can also control the reduction rate of the silver ions and the aggregation process of silver atoms. In practice, the reduction can take place after the interaction between the silver

moiety and PVP. In this case, a complex between silver ions and PVP is formed, followed by the reduction of the silver atoms on the PVP.²⁷⁻³⁰

In previous studies, a silver alkylcarbamate complex was heated at 130 °C for a few minutes, resulting in its quantitative conversion to silver nanoparticles, carbon dioxide, and alkyl amine.²⁰⁻²⁶ Herein, we report a convenient procedure for the *in situ* preparation of Ag/PVP nanocomposites. In the absence of any solvent and reducing agent, the reduction of silver *n*-propylcarbamate (Ag-PCB) complex and radical polymerization of the monomer occurred simultaneously *via* heat treatment at temperatures as low as 110 °C. Moreover, important advantages of the *in situ* synthesis are that no additives (e.g. solvent, surface-active agent and reductant of metallic ions) are used, and that the stable silver colloid solution can be directly prepared in high concentration by simply dissolving solid Ag/PVP nanocomposites in various organic solvent.

Experimental Section

Materials and measurement. Silver *n*-propylcarbamate complex solution (13.86% *n*-propylamine/methanol (w/w = 50/20) solution) was prepared by a previously reported method.¹⁸ *N*-Vinylpyrrolidone (NVP) and lauryl peroxide (Aldrich Chem. Co.) were used as received. For the characterization of the silver nanoparticles and films, TEM (transmission electron microscope, a JEOL electron microscope (JEM-2000EXII)), UV-vis (Shimadzu, UV-1601PC spectrometer) and FT-IR spectroscopy were employed. XRD (X-Ray diffractometer) patterns of the Ag nanoparticle were measured using a Shimadzu XD-D1 X-ray diffractometer with CuK_α radiation ($\lambda = 1.54056 \text{ \AA}$) at a scanning rate of 2 degrees per second, in 2θ ranging from 10° to 90°. The ethanol solution used for dispersing the silver nanoparticles was dried slowly on amorphous carbon supported on a copper

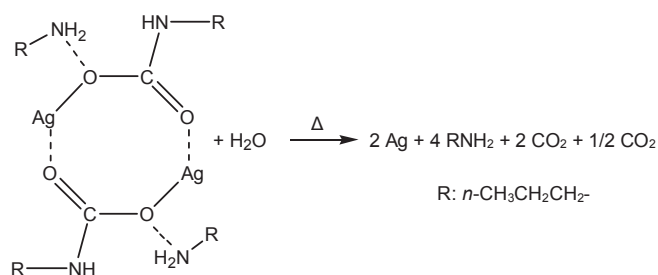
mesh TEM grid. The particle sizes of the nanoparticles were determined by directly measuring the sizes of 5 - 50 nm nanoparticles chosen randomly from the TEM images. TG/DTA (thermogravimetric/differential thermal analysis) measurement of silver carbamate complex solution was performed on a universal V4 2E TA instruments (SDT Q600 V8.2) under nitrogen at a heating rate of 10 °C/min. TGA (thermogravimetric analysis) measurement was performed on a Shimadzu TGA 50 thermal analyzer at a heating rate of 10 °C/min under nitrogen.

Preparation of Ag/PVP nanocomposites. Ag-PCB complex solution (2.0 g) was placed in a round-bottomed flask (50 mL) and the solvent was evaporated under reduced pressure at 20 °C. The resulting Ag-PCB complex (1.0532 g) and lauryl peroxide (10 mg) were directly dissolved in NVP monomer (5 g) at room temperature. The solution was degassed by high vacuum and then flushed with argon gas. The flask was heated to 110 °C and maintained at this temperature for 24 h. The resultant bulk product was taken out from the flask and heated at 130 °C for 30 min so as to remove the residual *n*-propylamine. The pure PVP was also prepared using a procedure similar to that described above.

Preparation of Ag/PVP nanocolloid solution. Nanocolloidal dispersions of PVP-protected silver in ethanol were prepared by dissolving the Ag/PVP composite (2 g) in ethanol (50 mL) under magnetic agitation for 5 min. The stability of the final produced silver colloid solution was measured by keeping the solution for 30 days at room temperature.

Results and Discussion

The thermal characterizations for the silver carbamate complex solution are shown in Figure 1. The DSC thermal profile and shows endothermic peaks at about 44.8 °C and 70.03 °C due to the evaporation of *n*-propylamine and methanol solvent. An additional endothermic peak observed at around 122.62 °C could be due to the decomposition of silver carbamate complex to give silver metal, carbon dioxide and *n*-propylamine as shown in Scheme 1. The TGA and DSC curve showed no heat flow changes up to 132 °C, which confirms that no volatile product was evolved while silver metal was formed. The TGA profile and differential curve for weight vs. temperature (Figure 1(b)) showed three distinct steps for weight loss up to 132 °C, indicating the possibility of three types of decomposition corresponding to the DSC curve. The TGA profile showed that up to ca. 70 °C there was 60% weight loss due to the evaporation of *n*-propylamine and methanol. The secession of chelated organic amine and the decomposition of silver carbamate bond occurred in



Scheme 1

succession. There was no loss up to 132 °C due to the formation of pure silver metal. The total weight loss was 86.14%, resulting in 13.86% silver content. The exothermic peak at 244.72 °C was caused by the agglomeration of silver nanoparticles.

TGA using isothermal aging method after an incremental temperature increase from 28 to 110 °C showed a 13.86% residual weight after 20 min as shown in Figure 2. Therefore, the silver carbamate complex can be decomposed to silver metal after aging at 110 °C within 20 min.

The formation of silver may be explained as follows. It has been shown that silver carbamate complex can be decomposed to form silver metal by only heat treatment at temperatures in the range of 70 to 130 °C. As is well known, the decomposition reaction of silver alkylcarbamate may be represented as follows: $2 \text{Ag}_2(\text{OCONHC}_3\text{H}_7) \cdot 2 \text{C}_3\text{H}_7\text{NH}_2 + \text{H}_2\text{O} \rightarrow 2 \text{Ag} + 4 \text{C}_3\text{H}_7\text{NH}_2 + 2 \text{CO}_2 + 1/2 \text{O}_2$. This reaction indicates that Ag-PCB is reduced to metallic silver simply by heating, and that the reaction is accompanied by the formation of *n*-propylamine and release of carbon dioxide. The Ag/PVP nanocomposites were prepared *via*

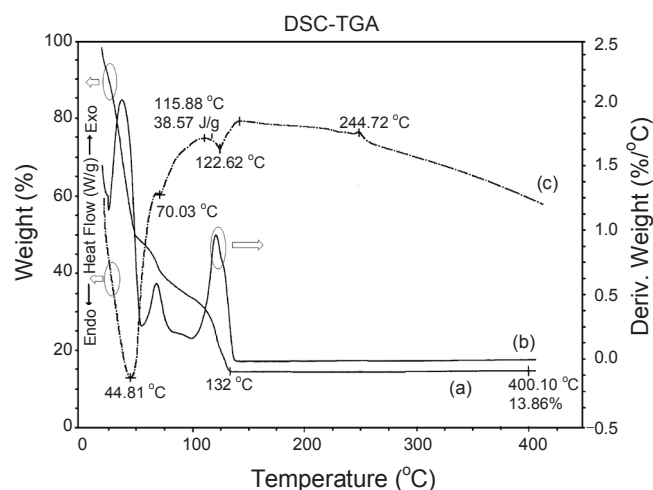


Figure 1. (a) TGA, (b) differential curve for weight/temperature and (c) DSC profiles of Ag-PCB complex solution.

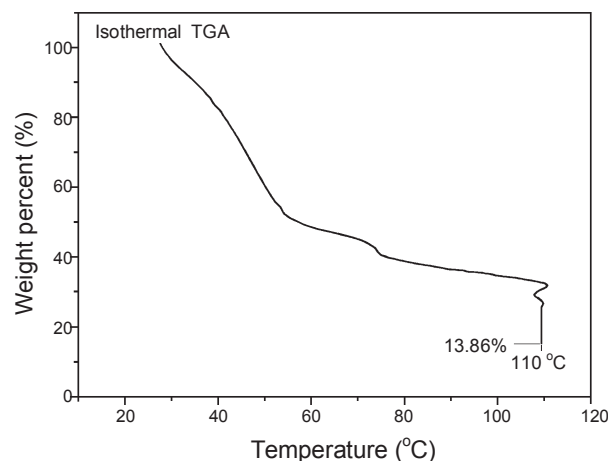


Figure 2. TGA thermogram of Ag-PCB complex solution using isothermal aging up to 110 °C.

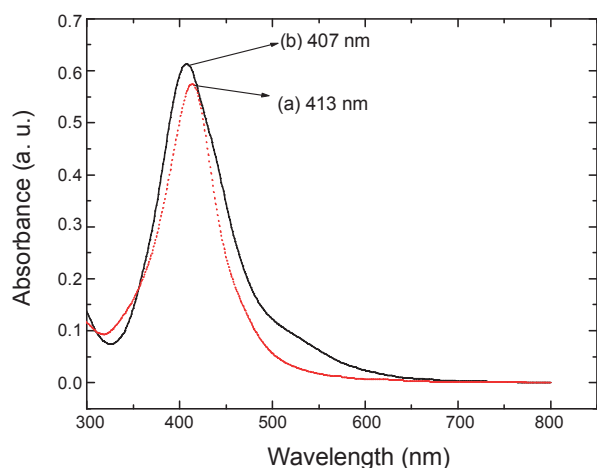


Figure 3. UV-vis absorption spectra of silver nanoparticle in (a) NVP and (b) PVP (solution in ethanol).

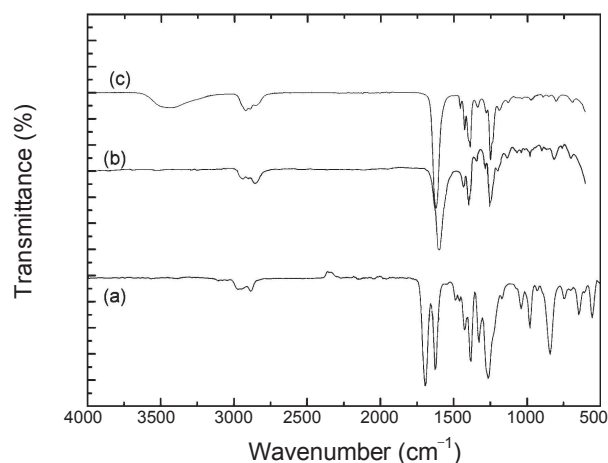


Figure 5. FT-IR spectra of (a) NVP, (b) PVP and (c) Ag/PVP composite.

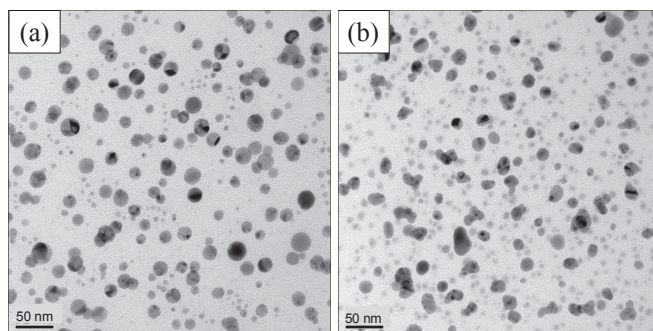


Figure 4. TEM image of silver nanoparticle dispersed in (a) NVP and (b) PVP (solution in ethanol); Scale bar (50 nm).

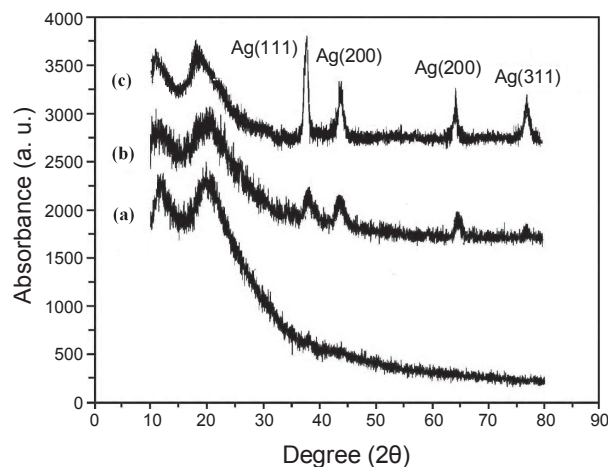


Figure 6. The XRD patterns of (a) PVP, (b) Ag/PVP (w/w = 99/1) and (c) Ag/PVP (w/w = 90/10) composites.

the radical polymerization with lauryl peroxide as a radical initiator only by heating at 110 °C. Since reduction and polymerization occur simultaneously, the resulting silver nanoparticles can be spontaneously dispersed in the PVP matrix. Further, the narrow particle size distribution suggests that the solubility of the complex of Ag-PCB in the NVP monomers plays an important role in the particle size distribution.

When an ampoule containing an *N*-vinylpyrrolidone (NVP) solution of Ag-PCB was heated to 110 °C for 20 min without a radical initiator, the precursor solution quickly turned dark and then gradually changed into a brown color. Figure 3(a) shows the UV-vis spectrum of the silver nanoparticle suspension obtained from the solution of Ag nanoparticles in the NVP monomer. An absorption peak at 413 nm was observed, which is attributed to the surface plasmon resonance of silver nanoparticles. When the polymerization proceeded, a somewhat broad UV absorption band centered at 407 nm as shown in Figure 3(b). Moreover, a blue shift in the maximum of the plasmon peak occurred. These features are associated with the better stabilizing effect of PVP than that of NVP. It was well known that polymers, as protecting agents, are very effective to inhibit the agglomeration of particles.

Figure 4(a) shows the TEM image of the silver nanoparticles prepared in NVP solution by heating at 110 °C after 20 min. The particles were spherical in shape, with a narrow size distribution

ranging from 5 to 25 nm. The Gaussian fit shows that the mean diameter of the particles is 18.7 nm and the fitted standard deviation is 5.0. Figure 4(b) shows a TEM image of the silver/PVP nanocomposites prepared during the radical polymerization after dissolving in alcohol solvent. Dark brown colloidal silver dispersions were obtained, exhibiting average diameters of from about 2 to 30 nm (mean diameter, 13.3 nm). The heating caused simultaneous reduction of the silver alkylcarbamate complex and radical polymerization of the monomer.

FTIR analysis was employed to examine the formation of the silver/PVP nanocomposites, as shown in Figure 5. The FTIR measurement of the silver carbamate complex and NVP solution showed that the band assigned to the carbon-carbon double bond stretching band of NVP at 1620 cm⁻¹ disappeared after heating at 110 °C for 24 h, confirming the completion of polymerization. The characteristic band at 1670 cm⁻¹ corresponding to the C=O stretching of the pyrrolidinone ring exhibited without change. The frequency of the carbonyl stretching in the silver/PVP nanocomposites is broadened and shifted from 1670 to 1645 cm⁻¹. This shift of the carbonyl stretching band is associated with the

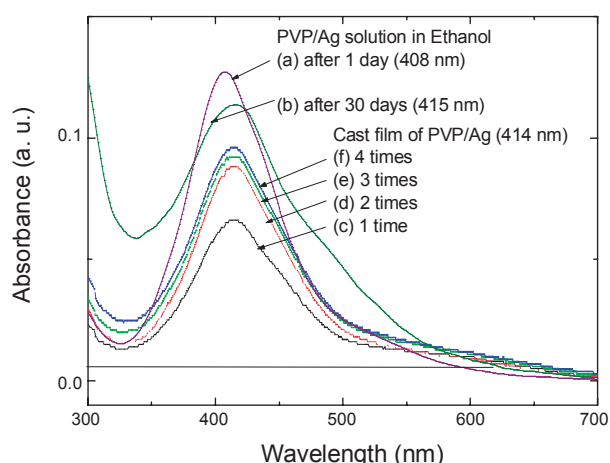


Figure 7. UV-vis absorption spectra of PVP protected silver nanoparticle solution synthesized from 2 g of Ag/PVP nanocomposites dissolved in ethanol after (a) 1 day, (b) 30 days and cast film (c) 1 time, (d) 2 times, (e) 3 times and (f) 4 times.

formation of a coordination bond between the silver atom and oxygen atoms in the carbonyl group.

The phase structures of the obtained silver/PVP composites were characterized by XRD analysis, as shown in Figure 6. The XRD pattern of pure PVP contains broad and sharp crystalline peaks (12° and 21°) as shown in Figure 6(a). However, the Ag/PVP nanocomposites (Ag/PVP Ag/PVP = w/w, 1/99 and 10/90) exhibits a two-phase structure in its XRD pattern, as shown in Figure 6(b) and 6(c). Besides the diffraction peaks of the PVP phase, the other peaks at 38.00° , 44.4° , 64.5° and 77.5° are in good agreement with the literature values of silver nanoparticles.³¹ These peaks are indexed to the (111), (200), (220), and (311) planes, respectively, representing the face-centered cubic (fcc) phase of silver. These results indicate that silver nanoparticles were prepared directly in the polymerization mixture containing the silver carbamate complex simply by heating.

To monitor the stability of the final produced silver colloid obtained from solid Ag/PVP nanocomposites, the change in time for the absorption spectra of the colloid on different days was measured. Figure 7(c)-(f) show the UV-vis spectra of the Ag/PVP films cast from the ethanol solution of the Ag/PVP nanocomposites. These spectra are different from that of the ethanol solution of the Ag/PVP nanocomposites as shown in Figure 7(a). The shifts in absorption wavelength when compared to its solution counter are normal observations as during the film formation the particle size generally increase. The spectrum shows an absorption peak centered at 414 nm, with a bandwidth of 81 nm at half-maximum height. The position of this peak occurs in the same region where PVP-protected silver colloids show strong absorption in both diluted and concentrated solutions: at 407 nm in 9.0% solution in ethanol. After 30 days of agitation, the characteristics of the silver nanoparticles change in the position, shape, and symmetry of the absorption spectra: the maximum absorbance showed a small red shift to 415 nm in position but the full width of half maximum increases to 135 nm as shown in Figure 7(b). The increase in maximum absorbance after 30 days of reaction in this system may be explained by an

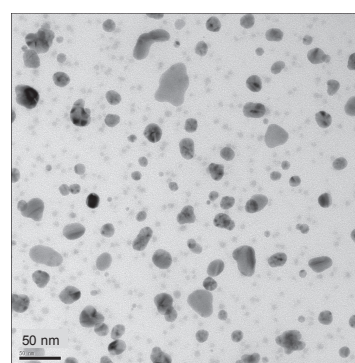


Figure 8. TEM image of silver nanoparticle in ethanol synthesized from 2 g of Ag/PVP nanocomposites dissolved in ethanol after 30 days; Scale bar (50 nm).

increase in particle coagulation.

Figure 8 shows a transmission electron micrograph showing that the nanoparticles obtained from dissolving the Ag/PVP nanocomposites in ethanol have an average particle size of 29.8 nm, with a standard deviation of 5.1 nm. The silver colloid grows from 5 - 25 to 10 - 40 nm and has a wider distribution than that of silver nanocolloid solution obtained after 1 day, coinciding with plasmon absorption spectra. However, at a high Ag/PVP concentration, the primary particles protecting the PVP polymer layer may potentially prevent significant aggregation.

Conclusion

Ag/PVP nanoparticle composites were prepared by the simultaneous thermal reduction and radical polymerization route. Silver nanoparticles with a narrow size distribution were obtained, which were well dispersed in the PVP matrix (up to 10 wt %). The synthesis proceeds successfully upon simple heat treatment at temperatures as low as 110°C . Moreover, important advantages of the *in situ* synthesis are that no additives (e.g. solvent, surfactant and reductant of metallic ions) are used, and that the stable silver colloid solution can be directly prepared in high concentration only by dissolving solid Ag/PVP nanocomposites in organic solvent. Therefore, the product may be directly used for industrial purposes.

References

- Volokitin, Y.; Sinzig, J.; de Jongh, L. J.; Schmid, G.; Vargaftik, M. N.; Moiseevi, I. I. *Nature* **1996**, *384*, 621.
- Flitton, R.; Johal, J.; Maeda, S.; Armes, S. P. *J. Colloid Interface Sci.* **1995**, *173*, 135.
- Zhong, J.; Wen, W. Y.; Jones, A. A. *Macromolecules* **2003**, *36*, 6430.
- Odegard, G. M.; Clancy, T. C.; Gates, T. S. *Polymer* **2005**, *46*, 553.
- Boev, V. I.; Pérez-Juste, J.; Pastoriza-Santos, I.; Silva, C. J. R.; de Jesus, M.; Gomes, M.; Liz-Marzán, L. M. *Langmuir* **2004**, *20*, 10268.
- Fudouzi, H.; Xia, Y. *Langmuir* **2003**, *19*, 9653.
- Lu, Y.; Liu, G. L.; Lee, L. P. *Nano Lett.* **2005**, *5*, 5.
- Laine, R. M.; Choi, J.; Lee, I. *Adv. Mater.* **2001**, *13*, 800.
- Zhu, M. Q.; Wang, L. Q.; Exarhos, G. J.; Li, A. D. Q. *J. Am. Chem. Soc.* **2004**, *126*, 2656.

10. Zhang, Z.; Zhang, L.; Wang, S.; Chen, W.; Lei, Y. *Polymer* **2002**, *42*, 8315.
 11. Wada, Y.; Kobayashi, T.; Yamasaki, H.; Sakata, T.; Hasegawa, N.; Mori, H.; Tsukahara, Y. *Polymer* **2007**, *48*, 1441.
 12. Huang, L. M.; Wen, T. C. *Mater. Sci. Eng. A* **2007**, *445-446*, 7.
 13. Ghosh, K.; Maiti, S. N. *J. Appl. Polym. Sci.* **1996**, *60*, 323.
 14. Hatchett, D. W.; Josowicz, M.; Janata, J.; Baer, D. R. *Chem. Mater.* **1999**, *11*, 2989.
 15. Huang, C. J.; Yen, C. C.; Chang, T. C. *J. Appl. Polym. Sci.* **1991**, *42*, 2237.
 16. Gotoh, Y.; Igarashi, R.; Ohkoshi, Y.; Nagura, M.; Akamatsu, K.; Deki, S. *J. Mater. Chem.* **2000**, *11*, 2548.
 17. Dearden, A. L.; Smith, P. J.; Shin, D. Y.; Reis, N.; Derby, B.; O'Brien, P. *Macromol. Rapid Commun.* **2005**, *26*, 315.
 18. Alessio, R.; Dell'Amico, D. B.; Calderazzo, F.; Englert, U.; Guarini, A.; Labella, L.; Strasser, P. *Helv. Chim. Acta* **1998**, *81*, 219.
 19. Dell'Amico, D. B.; Calderazzo, F.; Labella, L.; Marchetti, F.; Pampaloni, G. *Chem. Rev.* **2003**, *103*, 3857.
 20. Park, M. S.; Lim, T. H.; Jeon, Y. M.; Kim, J. G.; Joo, S. W.; Gong, M. S. *Macromol. Res.* **2008**, *16*, 308.
 21. Park, M. S.; Lim, T. H.; Jeon, Y. M.; Kim, J. G.; Joo, S. W.; Gong, M. S. *Sens. Actuators B* **2008**, *133*, 166.
 22. Park, M. S.; Lim, T. H.; Jeon, Y. M.; Kim, J. G.; Joo, S. W.; Gong, M. S. *J. Colloid Interface Sci.* **2008**, *321*, 60.
 23. Lim, T. H.; Jeon, Y. M.; Gong, M. S. *Polymer(Korea)* **2009**, *33*, 33.
 24. Jeon, Y. M.; Cho, H. N.; Gong, M. S. *Macromol. Res.* **2009**, *17*, 2.
 25. Hong, H. K.; Gong, M. S.; Park, C. K. *Bull. Korean Chem. Soc.* **2009**, *30*, 2669.
 26. Park, H. S.; Park, H. S.; Gong, M. S. *Polymer(Korea)* **2010**, *34*, 144.
 27. Huang, H. H.; Ni, X. P.; Loy, G. L.; Chew, C. H.; Tan, K. L.; Loh, F. C.; Deng, J. F.; Xu, G. Q. *Langmuir* **1996**, *12*, 909.
 28. Carotenuto, G. *Appl. Organometal. Chem.* **2001**, *15*, 344.
 29. Kapoor, S. *Langmuir* **1998**, *14*, 1021.
 30. Sarkar, A.; Kapoor, S.; Mukherjee, T. *J. Phys. Chem. B* **2005**, *109*, 7698.
 31. Monti, O. L. A.; Fourkas, J. T.; Nesbitt, D. J. *J. Phys. Chem. B* **2004**, *108*, 1604.
-